euronoise 2021
25th to 27th of October
Madeira, Portugal - online

On the Estimation of Directional Decay Times in Reverberation Rooms

Marco Berzborn, Jamilla Balint, and Michael Vorländer

Institute for Hearing Technology and Acoustics, RWTH Aachen University, 52074 Aachen

marco.berzborn@akustik.rwth-aachen.de

Abstract
The measurement of the random incidence absorption coefficient in a reverberation room according to the international standard ISO 354 requires a uniform damping of the modes of vibration composing the sound field. This requirement is violated when an absorbing specimen is mounted inside the room, resulting in decay curves with characteristic multi-exponential slopes when measured with an omni-directional microphone.
In this contribution we investigate the directional distribution of decay times of corresponding modes with respect to their direction of propagation. The sound field is decomposed into its two-dimensional angular wave number spectrum implicitly approximating the modes of vibrations as superposition of plane waves, followed by Schroeder integration for each direction. Decay times are estimated from the respective directionally dependent Schroeder integral and their distribution is compared to the reverberation times inferred from the omni-directional decay curve using Bayesian statistics. Experimental results for a rectangular reverberation room indicating an anisotropic sound field decay as well as non-uniform angular distribution of decay times are presented.

Keywords: Absorption, sound field decay, spherical arrays, directional decay

1 Introduction

The random-incidence absorption coefficient measured in a reverberation room imposes the requirements of an isotropic and homogeneous sound field as well as an uniform damping of the modes constituting the latter. Both requirements are expected to be violated during absorption coefficient measurements, at the latest when a test specimen is placed in the room [1, 2]. Even though many efforts have been made to counteract this problem –mostly involving attempts to increase the diffusion of the sound field by introducing scattering elements into the laboratory room – the issue still remains resulting in a poor reproducibility across different laboratories [3]. Based on analytic investigations for rectangular rooms Hunt et al. [1] showed that axial, tangential, and oblique modes inherit different damping constants for uniform and non-uniform distributions of boundary conditions. They further showed that two groups of modes with distinctively different damping constants remain, if a single surface is covered with an absorbing material, that is the groups with grazing and non-grazing incidence onto the absorbing material. Kuttruff [4] later concluded that the energy decay curve (EDC) can be calculated as the Laplace transform of the damping distribution, giving examples of distributions resulting in multi-exponential EDCs. More recently, Nilsson [5] showed that the resulting EDC in a room with absorption concentrated on a single surface is governed by two decay constants. This was also found by Balint et al. [6] who used a Bayesian framework to estimate the decay constants from EDCs measured in a reverberation room. However both methods lack spatial information about the damping of modes.
In [7, 8] the authors presented the directional energy decay curve (DEDC) – calculated as the Schroeder integral evaluated on a plane wave decomposition of the sound field – for the analysis of sound field isotopy during the decay process, giving insights into the angular uniformity of energy decay in the decaying sound field. This contribution investigates the angular distribution of average decay times of modes grouped according to their direction of propagation in the DEDC. It is expected that decay times of mode groups with a direction of

propagation parallel to the absorber are governed by a longer decay compared to modes at oblique incidence. We hypothesize that the omnidirectional EDC exhibits a multi-exponential slope, which reduces to a single-exponential slope when the sound field is decomposed with respect to aforementioned mode groups.
This contribution is organized as follows: The first section briefly introduces the concepts for the sound field decomposition and estimation of directional decay times using Bayesian statistics. The second section introduces the experimental setup in a reverberation room without any diffusing elements occupied with an absorber. The results and conclusions are presented in the last two sections of this paper.

2 Sound Field Analysis

2.1. Directional Energy Decay Curves

Spherical microphone arrays (SMAs) allow for the capture of directional room impulse responses (DRIRs) retaining angular information about the sound field in the room [9]. Assuming a sound field composed of plane waves, the sound pressure at the microphone positions of an SMA is found as [10]

$$\mathbf{p}(k) = \mathbf{B}(k)\mathbf{a_{nm}}(k), \tag{1}$$

where the matrix $\mathbf{B}(k)$ contains the angular as well as radial description of the array. The vector $\mathbf{a_{nm}}(\mathbf{k})$ contains the spherical harmonic (SH) coefficients defining the wave number dependent amplitude density of the plane wave sound field, also referred to as the spherical wave number spectrum [11]. By transforming $\mathbf{a_{nm}}(\mathbf{k})$ into the spatial domain and subsequently solving Eq. (1) we decompose the sound field into a continuum of Q plane waves [12]

$$\mathbf{a}(k) = \mathbf{Y}\mathbf{W_{nm}}\mathbf{B}^{\dagger}(k)\mathbf{p}(k), \tag{2}$$

where the $(.)^{\dagger}$ operator denotes the Moore-Penrose Pseudo-inverse and $\mathbf{Y}$ is the steering matrix of the array containing vectors of the SH basis functions evaluated at the q'th steering direction with elevation and azimuth angles (θ_q, ϕ_q), respectively. The diagonal matrix $\mathbf{W_{nm}}$ contains Dolph-Chebyshev weights [12] for uniform side-lobe attenuation. For a more in depth introduction into the required spherical array signal processing the reader is referred to the literature by Rafaely [12].
In the following the spherical wave spectrum is assumed to reflect a two-dimensional projection of the three-dimensional wave number spectrum of the modal sound field in a room as defined in Ref. [1]. In contrast to the full three-dimensional spectrum, the spherical wave spectrum depends on the position of the receiver in the room. While the superposition of plane waves is assumed to be a good approximation for the modal sound field in a room [13], this local approximation results in a loss of information on the absolute resonant frequency of the modes, but simply allows for separation in terms of the direction of propagation of the modes. Exemplarily, all axial modes in a rectangular room correspond to a sum of two plane waves traveling in the same respective directions.
To investigate the directional sound field decay we may finally calculate the DEDC as the Schroeder integral [14] of the time domain angular wave number spectrum [7, 8]

$$\mathbf{d}(t) = \int_t^{\infty} |\mathbf{a}(\tau)|^2 d\tau, \tag{3}$$

representing the decay of all modes corresponding to the respective directions (θ_q, ϕ_q).

2.2. Decay Time Estimation

Multi-exponential decay processes measured with an omni-directional receiver are described using the decay model by Xiang [15] as a sum of I distinctively different decay processes

$$\tilde{e}(t) = \sum_{i=1}^{I} A_i e^{\frac{-13.8 \cdot t}{T_i}}, \tag{4}$$

where A_i and T_i are the amplitudes and decay times of the respective decay processes. In this work we assume that the decay times correspond to two groups of modes: (1) with direction of propagation parallel to the absorber and (2) with an oblique incidence on the absorber. Assuming that the modes in every group share similar damping – an assumption which requires a convex room shape and boundary conditions without significant changes inside a band of frequencies – we may therefore assume that the DEDCs of single directions are governed by a joint mean decay time. As a result a first oder decay model is feasible for the estimation of the directional decay times if all remaining directions of incidence and therefore their corresponding modes are sufficiently suppressed. Consequently, the DEDC model reduces to

$$\tilde{d}(t, \theta_q, \phi_q) = A(\theta_q, \phi_q) e^{\frac{-13.8 \cdot t}{T(\theta_q, \phi_q)}}, \tag{5}$$

where $A(\theta_q, \phi_q)$ and $T(\theta_q, \phi_q)$ are the respective amplitudes and directional decay times.
The decay parameters of both models can be inferred using Bayesian statistics, where the relation between measurement and model is encoded into a Student-T distributed likelihood-function [15]. Given that the decay parameters follow a chosen prior distribution, their values can be estimated from their posterior distributions under the observation of the likelihood distribution, that is the measurement data and the model.[1] The underlying posterior distributions can be inferred using automated differentiation variational inference by maximizing the evidence lower bound [16]. The posterior distributions are approximated as full-rank Gaussian distributions, maintaining potential correlation between the model parameters. A set of most probable decay parameters can subsequently be extracted using bridge sampling [17].
While the use of a first order model as in Eq. (5) may initially seem equivalent to a linear regression in accordance with the international standard ISO 354 [18], it has to be stressed that the presented approach is different for two reasons. Firstly, the full dynamic range of the decay process is used, rather than omitting the initial 5 dB. Secondly, the Bayesian parameter inference avoids over-fitting and is numerically more robust [15].

3 Experimental Setup

The directional sound field decay was investigated experimentally in a rectangular reverberation room at the Technical University of Denmark (2800 Kgs. Lyngby, Denmark). For the present study all panel diffusers were removed, ensuring a well defined multi-exponential decay process. An absorbing sample of glass wool with a flow resistivity of $12.9\,\mathrm{kPa \cdot s/m^2}$, a thickness of 100 mm, and a surface area of $10.8\,\mathrm{m^2}$ was placed on the floor, a mounting frame was also omitted to avoid scattered reflections at its edges. The dimensions of the room are $(x, y, z) = (6.25\,\mathrm{m}, 7.85\,\mathrm{m}, 4.9\,\mathrm{m})$ with an approximate volume of $245\,\mathrm{m^3}$. A sequential dual-layer SMA centered at $(2.98\,\mathrm{m}, 4.16\,\mathrm{m}, 1\,\mathrm{m})$ (cf. Fig. 1) was sampled using a UR5 (Universal Robots, Odense, Denmark) scanning robot arm moving a pressure-field 1/2″ Brüel & Kjær type 4192 microphone. Each of the two radii ($r = (0.25\,\mathrm{m},\ 0.45\,\mathrm{m})$) contained 144 sampling positions distributed according to an equal-area partitioning [19] as well as additional sampling points inside each sphere for the stabilization of the eigenfrequencies of the sphere [20]. Impulse response measurements were performed with the ITA-Toolbox [21] using exponential sweeps driving a source mounted in the corner below the ceiling at approximately $(0.2\,\mathrm{m}, 0.2\,\mathrm{m}, 4.7\,\mathrm{m})$. The

[1] For an in depth derivation and explanation the reader is referred to the literature by Xiang et al. [15]

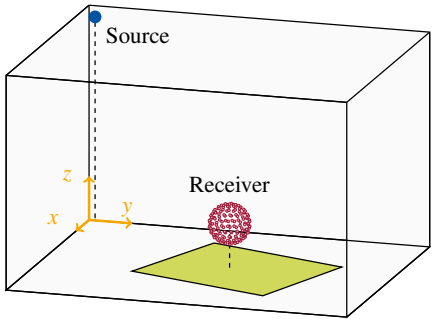

Figure 1: The experimental setup with source and receiver positions as well as the absorber position in the reverberation room. For better visual interpretation only sampling positions on the outer sphere are shown.

sampling duration was 2.5 h with temperature changes below 0.3 °C during the procedure.
The estimation of the angular wavenumber spectrum was performed for a SH order $N = 7$ for 200 steering directions on a uniform grid [19]. The Dolph-Chebyshev weights were chosen to achieve a side-lobe attenuation of 60 dB. The decay times $T(\theta_q, \phi_q)$ were estimated from the respective DEDCs using the *full-rank ADVI* algorithm implemented in the Python package *pymc3* [22]. To ensure computational feasibility of the parameter inference, all decay curves were downsampled to time steps of approximately 10 ms after Schroeder integration. While a first order model was assumed for the estimation of the directional decay times, a second order model was chosen for the estimation of decay times from the omnidirectional EDC. An assumption that is justified based on Bayesian evidence [15] and is in line with findings by Balint et al. [6]. In order to minimize local fluctuations in the decay process, the omnidirectional EDC was calculated by averaging the EDCs of all 310 microphone positions without any array processing applied.

4 Results

Figure 2 shows the omni-directional EDC for the third-octave bands 400 Hz (left) and 500 Hz (right), averaged over all 310 receiver positions. In both cases a double-sloped decay is present, therefore a multi-exponential decay model is applied to calculate the initial decay time T_1 and late decay time T_2. The Bayesian approach described in Section 2 is used to estimate the decay distribution as shown in Fig. 3. For the single value T_1 corresponding to the initial decay time, the mean value of the first distribution is calculated, for the late decay time it is done accordingly with the second distribution. For both frequency bands the initial decay time

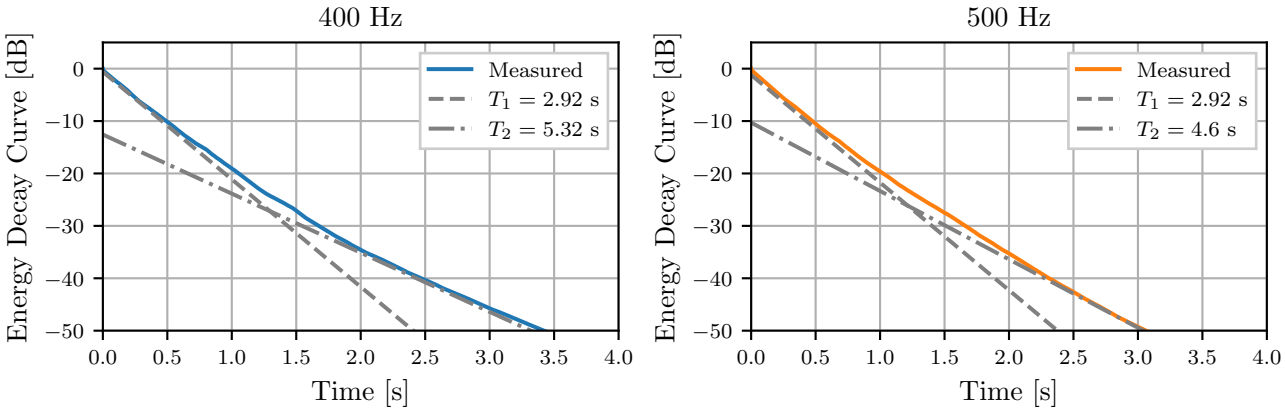

Figure 2: Measured omni-directional EDC, inital decay time T_1 and late decay time T_2.

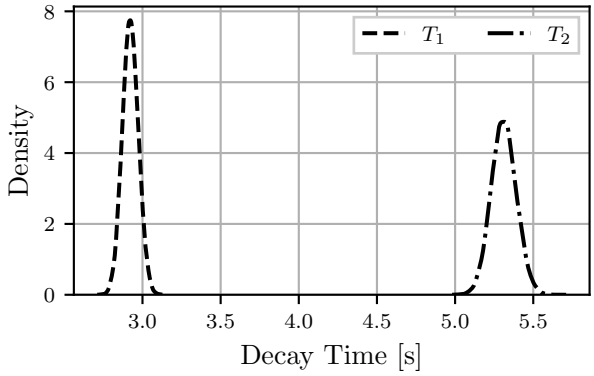

Figure 3: Decay time distribution for 400 Hz estimated with the Bayesian approach.

Table 1: Decay paramters T_1, T_2, T_{20}, and T_{30} for 400 Hz and 500 Hz.

	T_1	T_2	T_{20}	T_{30}
400 Hz	2.92 s	5.32 s	3.36 s	3.60 s
500 Hz	2.92 s	4.60 s	3.31 s	3.56 s

corresponds to $T_1 = 2.92$ s. The late decay times correspond to $T_2 = 5.32$ s and $T_2 = 4.6$ s for the 400 Hz and for 500 Hz bands, respectively. The clear double-sloped nature of the decay results from (a) the separation of the sound field due to non-uniform distribution of absorption in the reverberation room (grazing and non-grazing sound field in vertical and horizontal planes) and (b) the varying decay times within the frequency bands (grazing modes will exhibit a longer decay time as well as axial and tangential modes compared to oblique modes). The bending point of the decay curves are located between −20 dB and −30 dB, consequently applying linear regression in compliance with ISO 354 to calculate well-known reverberation parameter T_{20} or T_{30} lead to results which lie between the early and late decay values as shown in Table 1.

The directional energy distribution at 400 Hz for the steady-state condition and the time instances where the omni-directional EDC reaches −5 dB, −25 dB, and −35 dB are shown in Fig. 5, normalized by their mean value (the colors indicate the deviation from the mean). The plot is aligned with the coordinate system of the room in Fig. 1, hence the x-axis is indicated at 0° and 180° and the y-axis at - 90° and 90° in the azimuth direction. In the steady-state condition the energy is mainly concentrated in the upper hemisphere due to the high absorption on the ground, where the absorber is placed. The distinct maxima found in steady-state initially decrease, indicating an increased mixing of the sound field, which is in agreement with findings from a previous study where the authors found an initial increase in estimated isotropy during the initial decay process [8]. At the time instance where decay levels are at - 25 dB and - 35 dB a de-mixing of the sound field occurs and the energy is concentrated in the horizontal plane of the reverberation room. Eventually, at t_{-35dB}, distinct energy peaks are visible at 0° and 180°, indicating the presence of axial room modes in the x-direction.

Regions with higher energy levels during the decay process (cf. Fig. 4) correspond to the longer decay times shown in Fig. 5, where the directional decay times for the third-octave frequency bands of 400 Hz and 500 Hz are plotted. At 400 Hz a decay time up to 5.5 s is visible at 0° and 180°, indicating an axial mode in the x-direction. This is in line with the late decay time T_2 estimated from the omni-directional EDC. For the case of 500 Hz a longer decay time of 4.5 s is visible at 90°, indicating the presence of an axial mode in the y-direction, which again matches the late omni-directional decay time T_2. The shortest decay times which are located in the lower hemisphere in Fig. 5 should correspond to the the initial decay times estimated in Tab. 1, but are slightly overestimated (approximately 3.3 s instead of 2.9 s). Due to the room shape and absorber location a symmetry between upper and lower hemisphere is expected. This tendency is more distinct in the 400 Hz band than in the

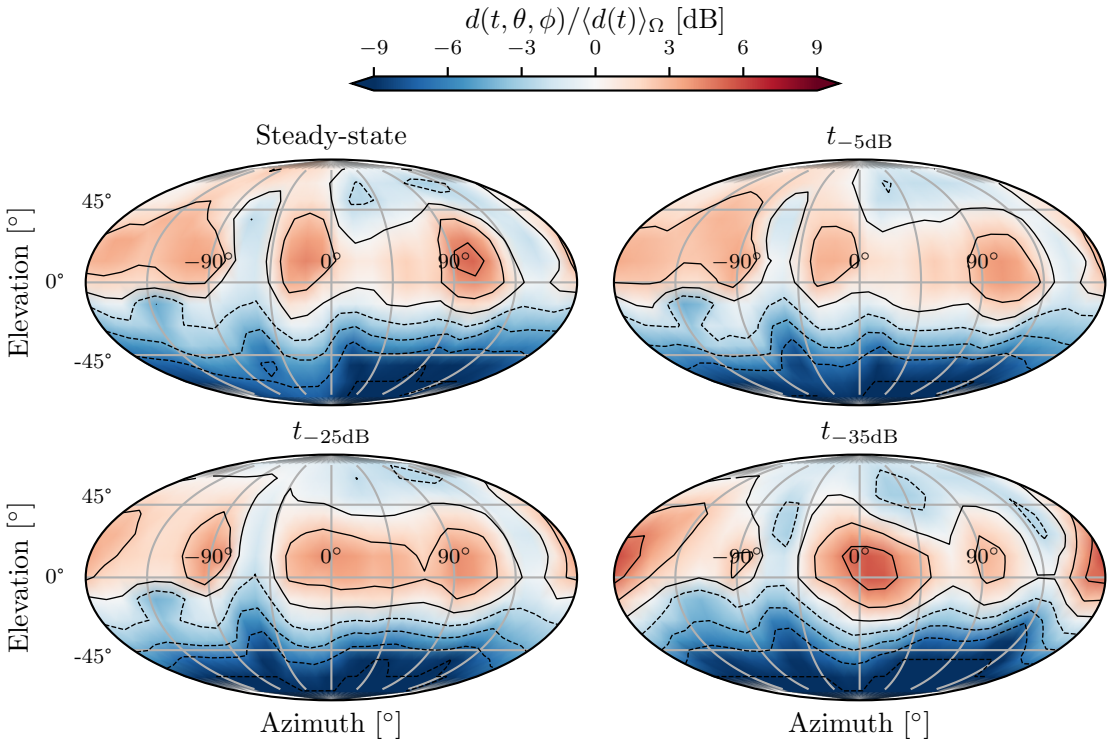

Figure 4: Directional energy decay curves normalized by their mean over all directions. The time instances correspond to the steady-state and omni-directional energy decays of −5 dB, −25 dB, and −35 dB.

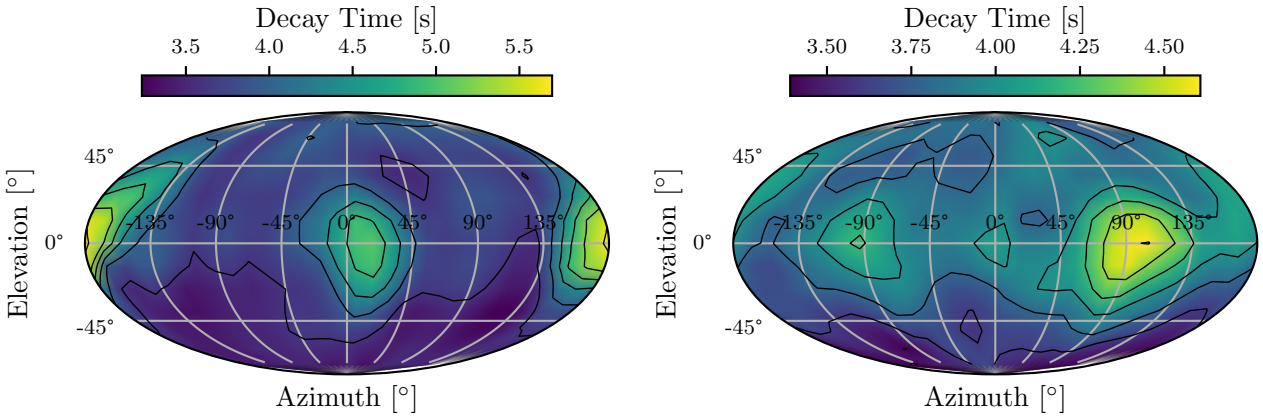

(a) 400 Hz

(b) 500 Hz

Figure 5: Directional decay times for the third-octave bands 400 Hz (left) and 500 Hz (right)

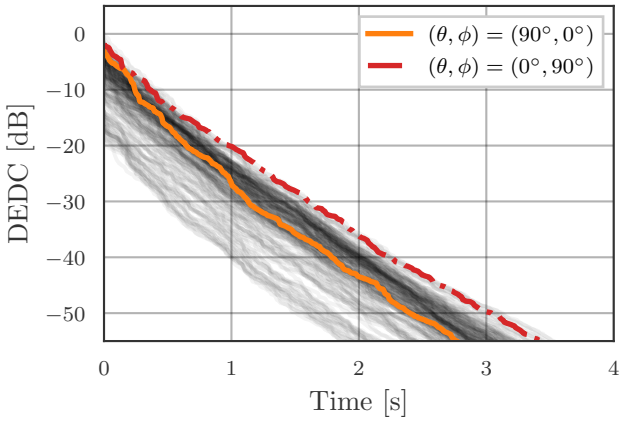

Figure 6: DEDCs at 500 Hz for 200 directions (–), for (90°, 0°) (–), and for (0°, 90°) (–·).

500 Hz band. However, for both bands, an overestimation of decay times is evident in the upper hemisphere, compared to the lower hemisphere. Reasons for the overestimation are discussed in the following paragraph.
In Fig. 6, the directional energy decay curves are shown for 200 directions. For the sake of illustration curves are highlighted for two directions: (90°, 0°) and (0°, 90°). Interestingly the DEDC for (90°,0°) clearly shows a multi-exponential behavior, although a single-exponential decay was expected if looking only into a certain direction. When estimating decay times one would have to use a multi-exponential model for a better representation of the data. However, applying a second order model resulted in inconclusive results, indicating an overfitting due to a mismatch between model and measured data. One reason for the presence of multi-exponential decays after sound field decomposition could be a non-ideal separation of the mode groups due to insufficient side-lobe attenuation and angular resoluton of the beamforming algorithm. The DEDC for (0°, 90°), which corresponds to a slowly decaying axial mode in the y-axis, exhibits a fairly straight decay. Hence, the decay time is in agreement with the late decay T_2 = 4.6 s, estimated with the Bayesian approach from the omni-directional EDC. In this case a first order model gives a good estimate for the decay time.

5 Conclusion

We presented an analysis of the directional energy decay process in a reverberation room with an absorbing sample placed on the floor. The presented method is based on the Schroeder integration of the plane wave decomposition of the sound field. Measurements were conducted without panel diffusers mounted in the room, giving rise to separate mode groups with direction of propagation parallel to the absorber and at oblique incidence, hence constituting a well comprehensible setup. Results indicate a non-isotropic sound field decay as well as a non-uniform angular distribution of decay times. Directions of dominating modes with long decay times could be identified parallel to the absorber. We further analysed the omni-directional EDC averaged over all receiver positions, showing that a multi-exponential decay model is needed to represent the decay process with an initial and late decay. The late decay time inferred from the omni-directional EDC was linked to the directions of axial modes when compared to the directional decay times inferred from the DEDC. A similar relationship was not fully established for the initial decay time estimated from the omni-dictional EDC, due to an overestimation of directional decay times. This mismatch primarily arises due to the insufficient side-lobe attenuation of the beamforming algorithm and therefore the non-ideal separation of the mode groups. A model including the beamformer directivity is required for future work. Nevertheless, it is expected that the presented method leads to an improved understanding of the directional properties of the sound field and its decay process – namely the lack of isotropy and the non-uniform damping of modes – and their effect on the measurement of the random incidence absorption coefficient.

Acknowledgements

The authors would like to thank Mélanie Nolan and Efren Fernandez-Grande for the collaboration on gathering the experimental data and many fruitful discussions, and Samuel A. Verburg for his help with the experimental setup. Work presented here was funded under DFG Grant VO 600 41-1.

References

[1] F. V. Hunt, L. L. Beranek, and D. Y. Maa. Analysis of Sound Decay in Rectangular Rooms. *J. Acoust. Soc. Am.*, 11(1):80–94, July 1939.

[2] Mélanie Nolan, Samuel A. Verburg, Jonas Brunskog, and Efren Fernandez-Grande. Experimental characterization of the sound field in a reverberation room. *J. Acoust. Soc. Am.*, 145(4):2237–2246, April 2019.

[3] R. E. Halliwell. Inter-laboratory variability of sound absorption measurement. *J. Acoust. Soc. Am.*, 73(3):880–886, March 1983.

[4] Heinrich Kuttruff. Eigenschaften und Auswertung von Nachhallkurven. *Acta Acust. United Ac.*, 8(4):273–280, 1958.

[5] Erling Nilsson. Decay Processes in Rooms with Non-Diffuse Sound Fields Part I: Ceiling Treatment with Absorbing Material. *Build. Acoust.*, 11(1):39–60, March 2004.

[6] Jamilla Balint, Florian Muralter, Mélanie Nolan, and Cheol-Ho Jeong. Bayesian decay time estimation in a reverberation chamber for absorption measurements. *J. Acoust. Soc. Am.*, 146(3):1641–1649, September 2019.

[7] Marco Berzborn and Michael Vorländer. Investigations on the Directional Energy Decay Curves in Reverberation Rooms. In *Proceedings of Euronoise*, pages 2005–2010, Hersonissos, Crete, 2018.

[8] Marco Berzborn, Mélanie Nolan, Efren Fernandez-Grande, and Michael Vorländer. On the Directional Properties of Energy Decay Curves. In *Proceedings of the 23rd International Congress on Acoustics*, pages 4043–4050, Aachen, Germany, 2019.

[9] Boaz Rafaely, Ilya Balmages, and Limor Eger. High-resolution plane-wave decomposition in an auditorium using a dual-radius scanning spherical microphone array. *J. Acoust. Soc. Am.*, 122:2661–2668, 2007.

[10] Boaz Rafaely. The spherical-shell microphone array. *IEEE/ACM Trans. Audio, Speech and Lang. Proc.*, 16(4):740–747, 2008.

[11] Earl G. Williams. *Fourier Acoustics*. Academic Press, 1st edition, 1999.

[12] Boaz Rafaely. *Fundamentals of Spherical Array Processing*, volume 8 of *Springer Topics in Signal Processing*. Springer-Verlag GmbH Berlin Heidelberg, 1st edition, 2015.

[13] A. Moiola, R. Hiptmair, and I. Perugia. Plane wave approximation of homogeneous Helmholtz solutions. *Z Angew Math Phys*, 62:809–837, 2011.

[14] M. R. Schroeder. New Method of Measuring Reverberation Time. *J. Acoust. Soc. Am.*, 37(6):1187–1187, 1965.

[15] Ning Xiang, Paul Goggans, Tomislav Jasa, and Philip Robinson. Bayesian characterization of multiple-slope sound energy decays in coupled-volume systems. *J. Acoust. Soc. Am.*, 129(2):741–752, February 2011.

[16] Alp Kucukelbir, Dustin Tran, Rajesh Ranganath, Andrew Gelman, and David M. Blei. Automatic Differentiation Variational Inference. *J Mach Learn Res*, 18(1):430–474, 2017.

[17] Quentin F. Gronau, Alexandra Sarafoglou, Dora Matzke, Alexander Ly, Udo Boehm, Maarten Marsman, David S. Leslie, Jonathan J. Forster, Eric-Jan Wagenmakers, and Helen Steingroever. A tutorial on bridge sampling. *J. Math. Psychol.*, 81:80–97, December 2017.

[18] International Organization for Standardization. ISO 354:2003 - Measurement of sound absorption in a reverberation room, 2003.

[19] Paul Leopardi. A partition of the unit sphere into regions of equal area and small diameter. *Electron. T. Numer. Ana.*, 25(12):309–327, 2006.

[20] G. Chardon, W. Kreuzer, and M. Noisternig. Design of spatial microphone arrays for sound field interpolation. *IEEE J. Sel. Topics Signal Process.*, 9(5):780–790, 2015.

[21] Marco Berzborn, Ramona Bomhardt, Johannes Klein, Jan-Gerrit Richter, and Michael Vorländer. The ITA-Toolbox: An Open Source MATLAB Toolbox for Acoustic Measurements and Signal Processing. In *Proceedings of the 43rd Annual German Congress on Acoustics*, pages 222–225, Kiel, 2017.

[22] John Salvatier, Thomas V. Wiecki, and Christopher Fonnesbeck. Probabilistic programming in Python using PyMC3. *PeerJ Computer Science*, 2:e55, April 2016.